Zahn, R., Comas, M.C., and Klaus, A. (Eds.), 1999
Proceedings of the Ocean Drilling Program, Scientific Results, Vol. 161

37. PLANKTONIC $\delta^{18}O$ RECORDS AT SITES 976 AND 977, ALBORAN SEA: STRATIGRAPHY, FORCING, AND PALEOCEANOGRAPHIC IMPLICATIONS[1]

Rita von Grafenstein,[2] Rainer Zahn,[3] Ralf Tiedemann,[3] and Anne Murat[4]

ABSTRACT

Planktonic (*Globigerina bulloides*) isotope profiles were measured for the Pleistocene sections at Sites 976 and 977. Both sites are in the Alboran Sea at key positions for monitoring the Atlantic-Mediterranean water exchange through the Strait of Gibraltar. At Site 976 we used samples from composite depth sections of Holes 976B, 976C, and 976D. Site 977 is a single-hole site and the isotope record was measured along Hole 977A. Age models for both sites were developed by using biostratigraphic marker events (de Kaenel et al., Chap. 13, this volume) and by graphical correlation with the benthic isotope record from Atlantic Site 659. The time scales were fine-tuned by tuning the isotope records to the combined orbital target curves of precession and obliquity. The isotope records can be well dated back to stage 35 at Site 976 and stage 57 at Site 977. Further below, the structure of the isotope records is inconclusive but, based on biostratigraphy, the bases of the records have been tentatively assigned to stage 57 (Site 976) and stages 61 or 63 (Site 977). According to the age models, sedimentation rates at both sites are between 15–40 cm/k.y. Glacial-interglacial $\delta^{18}O$ amplitudes are high during the past 450 k.y. at both sites (3.0‰ to 3.5‰), likely revealing a rapid change of both surface-water salinities and temperatures. Spectral analyses for three separate time windows reveal distinct changes in spectral character at the main orbital frequencies. Precession-related control on climate and hydrography played an important role during the middle and late Pleistocene, whereas high-latitude obliquity forcing dominated the middle Pleistocene. The mid-Pleistocene shift to a dominant 100-k.y. periodicity does not appear before 500 k.y. in the Alboran Sea (i.e., 100 k.y. to 200 k.y. later than in the open ocean). High-amplitude $\delta^{18}O$ variations occur also on sub-Milankovitch time scales. Repeated deposition of organic-rich layers in the Alboran Sea was not only linked to insolation maxima and periods of planktonic $\delta^{18}O$ minima, but they occurred also during full glacial conditions and moderate insolation levels. This pattern is different from that of sapropel deposition in the eastern Mediterranean Sea and may be more closely linked to North Atlantic climate change and associated changes in the Atlantic inflow and atmospheric circulation.

INTRODUCTION

Understanding the water exchange between the Atlantic Ocean and Mediterranean Sea is of interest for paleoclimatologists and paleoceanographers. The water budget of the Mediterranean Sea is controlled by climatic conditions in the Mediterranean region that determine the hydrography of Mediterranean waters which, in turn, contribute to the North Atlantic salt budget by way of the saline Mediterranean outflow (Madelain, 1970; Béthoux, 1979; Reid, 1979; Zahn et al., 1987; Zenk et al., 1992).

Past variations from the modern anti-estuarine circulation (surface inflow, deep outflow) of Mediterranean water via the Strait of Gibraltar have been discussed since the early days of sapropel discovery in the eastern Mediterranean (Kullenberg, 1952). Since then, numerous studies have addressed the eastern Mediterranean sequences, but the climatic and hydrographic conditions that lead to the formation of sapropels are still under debate (e.g., Vergnaud-Grazzini et al., 1977; Cita et al., 1977, 1982; Rohling, 1994). Conceptual models that are discussed involve either enhanced surface productivity leading to a surplus of organic matter at the seafloor (Calvert et al., 1992; van Os et al., 1994) or anoxic bottom water conditions that would enhance organic carbon preservation (Olausson, 1961; Stanley, 1978; Williams et al., 1978; Sarmiento et al., 1988).

Sediment cores close to the Strait of Gibraltar are well suited for monitoring the evolution of the Atlantic-Mediterranean water exchange during the past. Paleoceanographic studies in the Alboran Sea and the Gulf of Cadiz so far have concentrated on the last glacial-interglacial period using mostly planktonic isotope profiles documenting glacial-interglacial $\delta^{18}O$ amplitudes that are higher than the global mean $\delta^{18}O$ change; distinct differences between glacial and interglacial microfaunal patterns are inferred to document changes in biological productivity (Vergnaud-Grazzini et al., 1986; Abrantes, 1988; Vergnaud-Grazzini and Pierre, 1991; Rohling et al., 1995; Troelstra and van Hinte, 1995). However, these data do not serve as unambiguous proof for a current reversal at the Strait of Gibraltar during the last deglaciation which has been proposed (e.g., Olausson, 1961; Stanley, 1978). Caralp (1988) compared late-glacial to recent benthic foraminifer assemblages on both sides of the Strait of Gibraltar and inferred a general evolution from a well-oxygenated, nutrient-rich environment during the Last Glacial Maximum to a nutrient-poor, oxygen-depleted environment from 13 ka to the present. An unusual assemblage with reduced species diversity between 10 ka and 7 ka, which is roughly coeval with sapropel S1 in the eastern Mediterranean, was assumed to indicate nutrient-poor, low-oxygenated conditions in the deeper parts of the Alboran basin (Caralp, 1988). This indicates reduced water exchange, but it is not clear evidence for a current reversal at the Strait of Gibraltar.

Trace-element patterns along sediment cores at both sides of the strait imply that the modern anti-estuarine circulation pattern persisted throughout the post-glacial sea-level rise (Grousset et al., 1988). During full-glacial conditions, advection rates of the deep outflow to the Atlantic were reduced in response to the glacially lowered sea level that caused the strait geometry to narrow (Béthoux, 1984; Bryden and Stommel, 1984). Isotope studies at the northeastern Atlantic

[1]Zahn, R., Comas, M.C., and Klaus, A. (Eds.), 1999. *Proc. ODP, Sci. Results,* 161: College Station, TX (Ocean Drilling Program).

[2]Paläontologisches Institut, Ludwig-Maximilians-Universität, München, Federal Republic of Germany. Rita.Grafenstein@cip.geo.uni-muenchen.de

[3]GEOMAR Research Center for Marine Geosciences, Kiel University, Federal Republic of Germany.

[3]Intechmer, BP 324, 50103 Cherbourg Cedex, France.

continental margins further suggest that the Mediterranean waters contributed to the North Atlantic hydrography during the last glacial, with sporadic reductions in advection during post-glacial sea-level rise (Zahn et al., 1987; Zahn et al., 1997).

The paleoceanographic program of ODP Leg 161 was dedicated to establish a long time series of paleoenvironmental records in the western Mediterranean Sea that would allow researchers to decipher its climatic and oceanographic evolution back to the Miocene. Alboran Sea Sites 976 and 977 were drilled to monitor the Pleistocene history of the Atlantic-Mediterranean water exchange. Site 976 is at a watchdog position ~110 km east of Gibraltar; Site 977 in the eastern Alboran Sea tracks the hydrography of Atlantic waters as they enter the southern Balearic Sea.

Herein, we present planktonic foraminiferal isotope records of Sites 976 and 977 that span the Pleistocene back to 1.4 Ma (Site 976) and 1.7 Ma (Site 977). The age models for both sites were developed using the biostratigraphic marker events of de Kaenel et al. (Chap. 13, this volume) and the benthic $\delta^{18}O$ record from eastern subtropical North Atlantic Site 659 of Tiedemann et al. (1994) for fine-tuning. High sedimentation rates up to 15–40 cm/k.y. permit detection of high-amplitude isotope variability both on Milankovitch (glacial-interglacial) and sub-Milankovitch time scales and to determine the stratigraphic position of organic-rich layers (ORL) at both sites (Murat, Chap. 41, this volume) in relation to orbital insolation cycles. Ultimately, this enables us to determine the timing of ORL formation in the westernmost Mediterranean Sea in relation to the timing of sapropel formation in the eastern Mediterranean and to draw conclusions regarding paleoceanographic conditions during ORL deposition.

SITE LOCATION AND OCEANOGRAPHIC SETTING

Site 976 is located in the western Alboran Sea, about 110 km east of the Strait of Gibraltar (36°12.3′N, 04°18.7′W) at a water depth of 1110 m. It is in the immediate neighborhood of DSDP Site 121 (Ryan et al., 1973). Three offset holes (Holes 976B, 976C, 976D) were used to construct a meter composite depth scale using color reflectance and magnetic susceptibility records (Comas, Zahn, Klaus et al., 1996). Site 977 is located in the eastern Alboran Sea (36°01.9′N, 01° 57.3′W), south of Cabo de Gata, at a water depth of 1984 m. Site 977 is a single-hole site that penetrated 598.5 m of Miocene/Pliocene to Holocene sediments.

Paleoceanographic objectives at both sites included retrieval of complete Pliocene–Pleistocene sedimentary sequences and Miocene deposits in the westernmost Mediterranean Sea near the Gibraltar Strait gateway. Paleoceanographic records from this region were expected to help monitor the hydrography of incoming Atlantic surface waters in relation to global climate. In particular, we hoped that the data would allow us to document the Atlantic-Mediterranean water exchange during the late Cenozoic and to decipher current patterns (i.e., potential switching between anti-estuarine and estuarine water flow through the Strait of Gibraltar).

Surface circulation of the Alboran Sea is dominated by two mesoscale gyres. The circulation in the western gyre (3°–5°W) is anticyclonic and mainly driven by bottom topography (Donde Va Group, 1984). The eastern gyre (1°–3°W) is mostly anticyclonic, but occasional cyclonic circulation has also been observed (Millot, 1987). A strong density front (Almería-Orán front) along its eastern boundary forces the Atlantic inflow to the south, forming a strong eastward jet through a narrow zone along the Algerian coast (Tintoré et al., 1994). Geostrophic forcing along the jet stimulates small-scale upwelling of deeper, nutrient-enriched waters that increase nutrients regionally in the surface layer, thus resulting in the development of regional high-productivity cells.

The hydrography of the Alboran Sea is determined by the low-salinity Atlantic surface inflow (S = 36.5) and the colder high-salinity (S > 38) outflow to the Atlantic at depth (Lacombe and Richez, 1982; La Violette, 1990). Changes in temperature and salinity of inflowing waters can be initially attributed to hydrographic changes in the North Atlantic (La Violette, 1990). Inflowing Atlantic water forms a low-density surface layer of 100–200 m thickness, the so-called Modified Atlantic Water (MAW; La Violette, 1994). Winter cooling in conjunction with enhanced evaporation resulting from an increased thermal offset between surface waters and air leads to an increase in MAW density.

Deeper water masses in the Alboran Sea are derived from sources in the western and eastern Mediterranean. Cold winds in late winter cause deep convection of waters in the Gulf of Lions (Lacombe, 1984) and the Liguro-Provençal Basin (Gascard, 1978) that form major contributions to the Western Mediterranean Deep Water (WMDW; MEDOC-Group, 1970). WMDW is present throughout the western Mediterranean Sea at depths between 800 and 3000 m (La Violette, 1994) and can be easily traced for its high salinity up to 38.4 (Rohling and Bryden, 1992). In the eastern Mediterranean, deep convection occurs in the Rhodes Gyre of the Levantine Sea and in the Adriatic Sea. In the Rhodes Gyre, dense Levantine Intermediate Water (LIW, T ≈15.5°C, S ≈39, potential density ≈28.95) is formed in response to enhanced evaporation and concomitant increase in surface salinity (Lascaratos et al., 1993; Wu and Haines, 1996). Eastern Mediterranean Deep Water (EMDW, T ≈13.6°C, S ≈38.7, potential density ≈29.13; Wu and Haines, 1996) is formed in the North Adriatic Sea, where LIW mixes with cold overlying subsurface water. EMDW formation occurs predominantly in winter, when cold and dry northeasterly "Bora" winds prevail (Wüst, 1961; Rohling, 1994; Wu and Haines, 1996). This water flows out via the Strait of Otranto into the Ionian Basin, where it sinks to below 2000 m and spreads to the south and east into the Levantine Basin (Wüst, 1961; Rohling, 1994; Wu and Haines, 1996). LIW also comprises an important contribution to WMDW.

The deep Mediterranean outflow layer in the Alboran Sea is largely derived from the upper layer of WMDW. The outflowing waters follow two separate paths, a deeper one at a more southerly position close to the Moroccan slope and a shallower one in the northern part of the Alboran Basin (Donde Va Group, 1984). The inflow-outflow exchange occurs in a three-layer flow system that has an active interface layer with variable thickness between the upper inflow and lower outflow layers (Bray et al., 1995). Mean volume transports are in the order of 1.04 Sv for inflowing Atlantic and 0.76 Sv for outflowing Mediterranean waters, the difference being attributed to evaporative water loss to the atmosphere (Bryden and Kinder, 1991a).

MATERIALS AND METHODS

We have generated planktonic isotope records for the Pleistocene sediment sections of Sites 976 and 977. The isotope measurements were carried out on 15–25 specimens of *Globigerina bulloides* d'Orbigny 1826 from the size fraction 250–355 µm. We chose this species because it is the only faunal constituent that is continuously available in sufficient numbers across glacial and interglacial sediment sections at both sites. All isotope samples were washed in methanol in an ultrasonic bath before isotope analysis. The isotope measurements were performed at the isotope laboratories of Bremen University (Site 976) and at GEOMAR (Site 977) on Finnigan MAT 251 and 252 mass spectrometers with single-sample "CARBO KIEL" carbonate preparation devices. The mass spectrometers at both laboratories are intercalibrated using the same internal carbonate standard (Solnhofen limestone). External precision of the measurements was better than 0.06‰ for $\delta^{18}O$ and better than 0.04‰ for $\delta^{13}C$, as shown by routine repeated analysis of the internal laboratory standard. All values were converted to the Pee Dee Belemnite (PDB) scales for carbonate $\delta^{18}O$ and $\delta^{13}C$.

For Site 976, the isotope record was established using samples from offset holes 976B, 976C, and 976D. Sampling of the three holes

followed the composite depth scheme given in Table 10 of the "Site 976" chapter in the Leg 161 *Initial Reports* volume (Comas, Zahn, Klaus, et al., 1996). The use of composite depth sections from the three holes helped to ensure continuity of the recovered sedimentary sequences and of the isotope record. Site 977 was a single-hole site, but there are only two minor gaps in the isotope record. To cover the Pleistocene sections at both sites, the upper 352.73 mcd (meters composite depth; equivalent to 348 mbsf, meters below seafloor) at Site 976 and the upper 271 mbsf at Site 977 were continuously sampled at 1-m intervals on average. Such a large sampling interval appeared sufficient for initial isotope analysis because shipboard biostratigraphy indicated that sedimentation rates are high at both sites (Comas, Zahn, Klaus et al., 1996), which is confirmed by postcruise refinement of the biostratigraphy (de Kaenel et al., Chap. 13, this volume). These estimates are largely confirmed by the isotope stratigraphies (see below). Mean sampling intervals in the upper 60 mbsf of Hole 976B, which was sampled on board *JOIDES Resolution*, was 40 cm. To establish the Pleistocene isotope records 367 and 291 isotope analyses were conducted on Sites 976 and 977, respectively. The isotope data from Sites 976 and 977 are available in Tables 1 and 2 on the CD-ROM, back pocket, this volume.

STRATIGRAPHY

Time Domain

The age models for Sites 976 and 977 were developed in three steps. As a first step, the depths and ages of biostratigraphic marker events from de Kaenel et al. (Chap. 13, this volume) were used as age fix points for the isotope records (Figs. 1, 2; Table 3). In a second step, the isotope records at Sites 976 and 977 were graphically correlated to the benthic isotope record and the astronomically calibrated time scale of Site 659 (Fig. 3; time scale from Tiedemann et al., 1994). For the graphical correlation we used the AnalySeries time series routine of Paillard et al. (1996). According to this correlation and the biostratigraphic marker events, isotope stages can be firmly assigned to the isotope records back to stage 35 (~1.23 Ma) at Site 976 and stage 57 (~1.64 Ma) at Site 977 (Figs. 1–3). A recovery gap at Site 976 from 280 to 295 mcd was probably caused by sediment loss caused by gas expansion of the sediments when the core was withdrawn from the seafloor. Between 295 and 320 mcd, the isotope record at Site 976 does not display the characteristic isotope fluctuations that are seen in the Site 659 record (Fig. 3). Below this section, the two isotope minima between 320 and 340 mcd (Fig. 1) have been correlated with isotope warm stages 51 and 53. The $\delta^{18}O$ minimum at the base of the record, between 350 and 355 mcd, has been tentatively assigned to isotope stage 57, largely on the basis of the marker ages for the first occurrence of *Gephyrocapsa* spp. (>5 µm; 348.63 mcd) at 1.61 Ma, the last occurrence of *Calcidiscus macintyrei* (349.32 mcd) at 1.619 Ma, and the first occurrence of *G. oceanica* (>4 µm; 361.05 mcd) at 1.718 Ma (de Kaenel et al., Chap. 13, this volume).

The $\delta^{18}O$ stage assignments at Site 977 (Fig. 2) are much better constrained because the structure of the early Pleistocene isotope record fits better to that of the Site 659 isotope record. Minor discrepancies between the Site 977 isotope curve and the Site 659 reference record exist between 1.2 and 1.3 Ma, where isotope warm stage 37 is not well developed in the Site 977 record. However, the $\delta^{18}O$ depletion during stage 37 at Site 659 is reduced compared to stage 37 isotope shifts documented at Pacific Sites 677 (Shackleton et al., 1990) and 849 (Mix et al., 1995) and, thus, the differences in isotope amplitudes likely are because of regional effects of temperature and/or seawater $\delta^{18}O$ in surface waters at Site 977. Accepting the biostratigraphic ages of 1.364 Ma for the base of the *Pseudoemiliania lacunosa* acme zone at 211.31 mbsf and of 1.512 Ma for the first occurrence of *G. oceanica* (>6.5 µm) at 231.48 mbsf (de Kaenel et al., Chap. 13, this volume; see Table 3), we infer a coring gap immediately above core break 24X/25X that spans isotope stages 47 and 48, which are apparently missing from the Site 977 isotope record. Below 256 mbsf, the structure of the isotope record is inconclusive. Using the biostratigraphic age of 1.719 Ma for the first occurrence of *G. oceanica* (>4 µm) at 262.73 mbsf, the $\delta^{18}O$ minimum at 264 mbsf may represent isotope warm stages 61 or 63.

In a third step, we refined the age models for Sites 976 and 977 by tuning the oxygen isotope records to two astronomically derived target curves. These curves (Fig. 3) were constructed by adding the normalized orbital signal of precession to one-half of that of obliquity

$$P + \left(-1 \times \frac{T}{2}\right) , \qquad (1)$$

where P is precession and T is tilt or obliquity. The target curves were derived from the astronomical solution $La90_{(1.1)}$ (Laskar et al., 1993), which was shown by Lourens et al. (1996) to be the most ac-

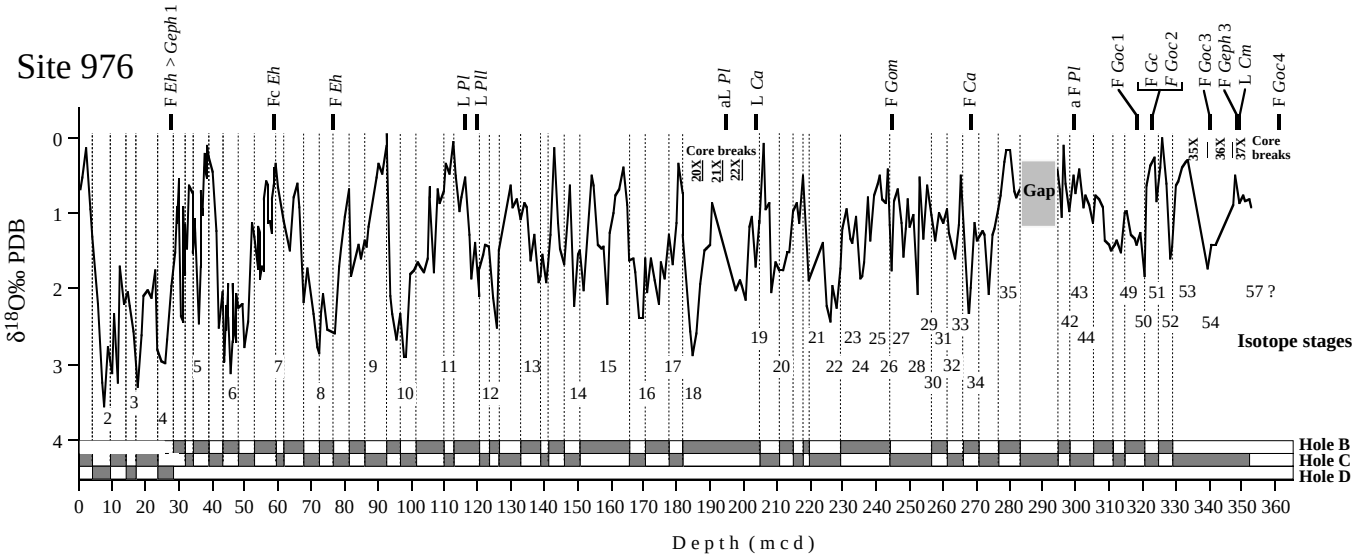

Figure 1. $\delta^{18}O$ profile of *G. bulloides* at Site 976. The depth scale is in meters composite depth (mcd). Switching between the three offset holes is indicated along the depth axis. Also shown are biostratigraphic marker events from de Kaenel et al. (Chap. 13, this volume). Between 181 and 204 mcd (Hole 976B) and 329 and 352 mcd (Hole 976C), core breaks are indicated above the isotope record. Numbers below the isotope record give oxygen isotope stage assignments.

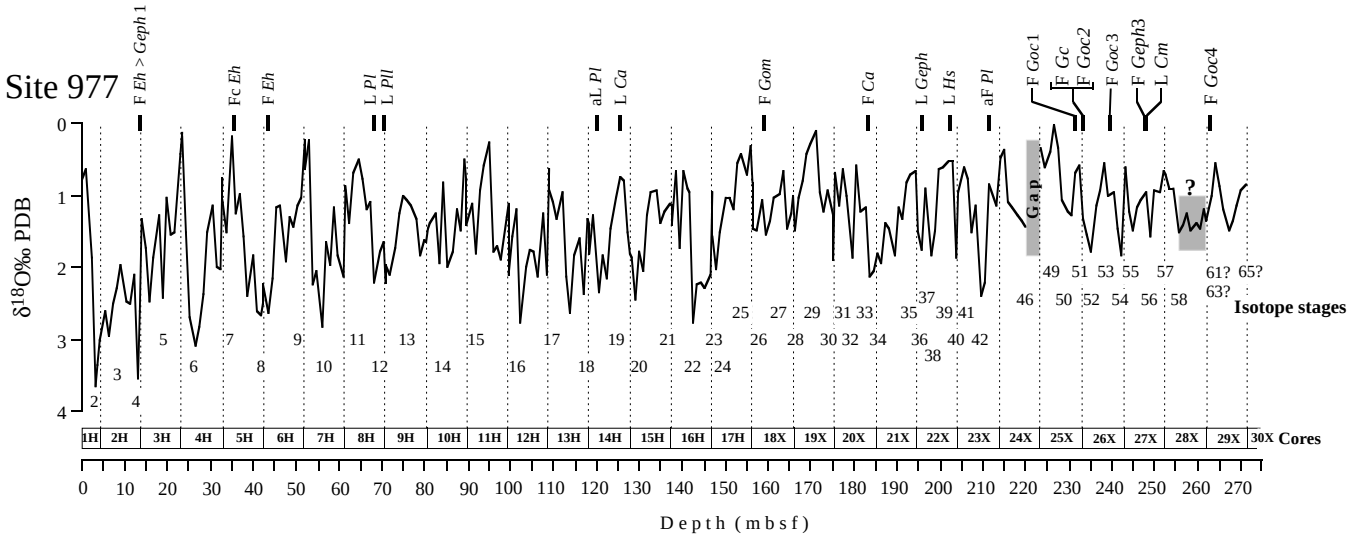

Figure 2. $\delta^{18}O$ profile of *G. bulloides* at Site 977. The depth scale is in meters below seafloor (mbsf). Cores and core breaks are indicated. Also shown are biostratigraphic marker events from de Kaenel et al. (Chap. 13, this volume). Numbers below the isotope record give oxygen isotope stage assignments.

Table 3. Biostratigraphic ages used to develop the initial age models at Sites 976 and 977.

		Hole 976B		Hole 977A	
Event code	Biostratigraphic event	Depth (mcd)	Age (ka)	Depth (mbsf)	Age (ka)
F *Eh* > *Geph* 1	FO *E. huxleyi* > *Gephyrocapsa* spp.	27.53	72.3	13.55	69.6
Fc *Eh*	FcO *E. huxleyi*	58.96	218.3	35.48	213
F *Eh*	FO *E. huxleyi*	76.55	270.54	43.55	268.5
L *Pl*	LO *P. lacunosa*	116.11	423.65	68.07	428.8
L *Pll*	LO *P. lacunosa lacunosa* (>7 µm)	119.75	438.8	70.3	454
aL *Pl*	acme LO *P. lacunosa*	194.48	747.29	120.29	752.8
L *Ca*	LO *C. asanoi* (cir.; >6.5 µm)	203.62	777.67	125.3	776.7
F *Gom*	FO *G. omega* (>4 µm)	244.31	962	159.03	976
F *Ca*	FO *C. asanoi* (cir.; >6.5 µm)	268.57	1121.73	183.08	1122
L *Geph* 2	LO *Gephyrocapsa* spp. (>6.5 µm)			195.71	1235
L *Hs*	LO *H. sellii*			202.24	1276
aF *Pl*	acme FO *P. lacunosa*	299.51	1361	211.31	1364
F *Goc* 1	FO *G. oceanica* (>6.5 µm)	318.375	1493	231.48	1512
F *Gc*	FO *G. caribbeanica* (>6.5 µm)	322.92	1516	233.55	1529
F *Goc* 2	FO *G. oceanica* (>6.3 µm)	322.92	1516	233.55	1529
F *Goc* 3	FO *G. oceanica* (>5.5 µm)	339.98	1569.7	239.81	1568
F *Geph* 3	FO *Gephyrocapsa* spp.(>5 µm)	348.63	1613	247.51	1614
L *Cm*	LO *C. macintyrei* (cir.; >11 µm)	349.32	1619	248.17	1619
F *Goc* 4	FO *G. oceanica* (>4 µm)	361.05	1718	262.73	1719

Notes: Biostratigraphic marker events are from de Kaenel et al. (Chap. 13, this volume). Marker events were determined for Hole 976B only. Comparison of the magnetic susceptibility records of Holes 976B and 976C, which were both used for the composite depth scheme, shows that the depth offset between the two holes remains nearly constant throughout the records. Hole 976B marker events may thus be readily transferred to Hole 976C by applying the depth offsets between both holes also to cores that are not in the composite depth scheme.

curate solution over the past 5.3 m.y. A second target record was generated by combining the normalized obliquity signal with one-half of the normalized precession signal

$$T + \left(-1 \times \frac{P}{2}\right) . \quad (2)$$

Inversion of the signals by factor –1 was needed to make both orbital signals climatically coherent. Before combining both signals, precession was lagged by 5 k.y. and obliquity by 8 k.y., applying phase lags between orbital insolation and ice volume response as inferred by Imbrie and Imbrie (1980) for the late Pleistocene. However, as discussed by Hilgen et al. (1993) and Lourens et al. (1996), these response times imply that the cyclic variations in the oxygen-isotope record are mainly driven by changes in global ice volume, which might not be true for the planktonic oxygen-isotope signal in the Mediterranean. They estimated a shorter precessional $\delta^{18}O$ lag time of Mediterranean surface-waters relative to precessional forcing of only 2–3 k.y. A shorter response time in the precessional $\delta^{18}O$ frequency band would reflect a predominant low-latitude climate forcing (e.g., by way of varying freshwater input from rivers in the Mediterranean borderlands). A presumed smaller phase difference in the precession band would result in only minor shifts of the tuned time scale, but that would impose more severe constraints on cross-spectral comparisons with high-latitude paleoceanographic records.

The orbital target records derived from Equations 1 and 2 (Fig. 3) were used alternatively depending on the variable stratigraphic resolution along both $\delta^{18}O$ records. The complete list of time scale fix points for both sites is given in Table 4.

Frequency Domain

To determine the spectral characteristics of the isotope records, we have run power spectra on the $\delta^{18}O$ records of Sites 976 and 977. Spectral analysis followed standard techniques described in Imbrie et al. (1992) using the ARAND spectral routines that were available from P.J. Howell at Brown University. The isotope records were

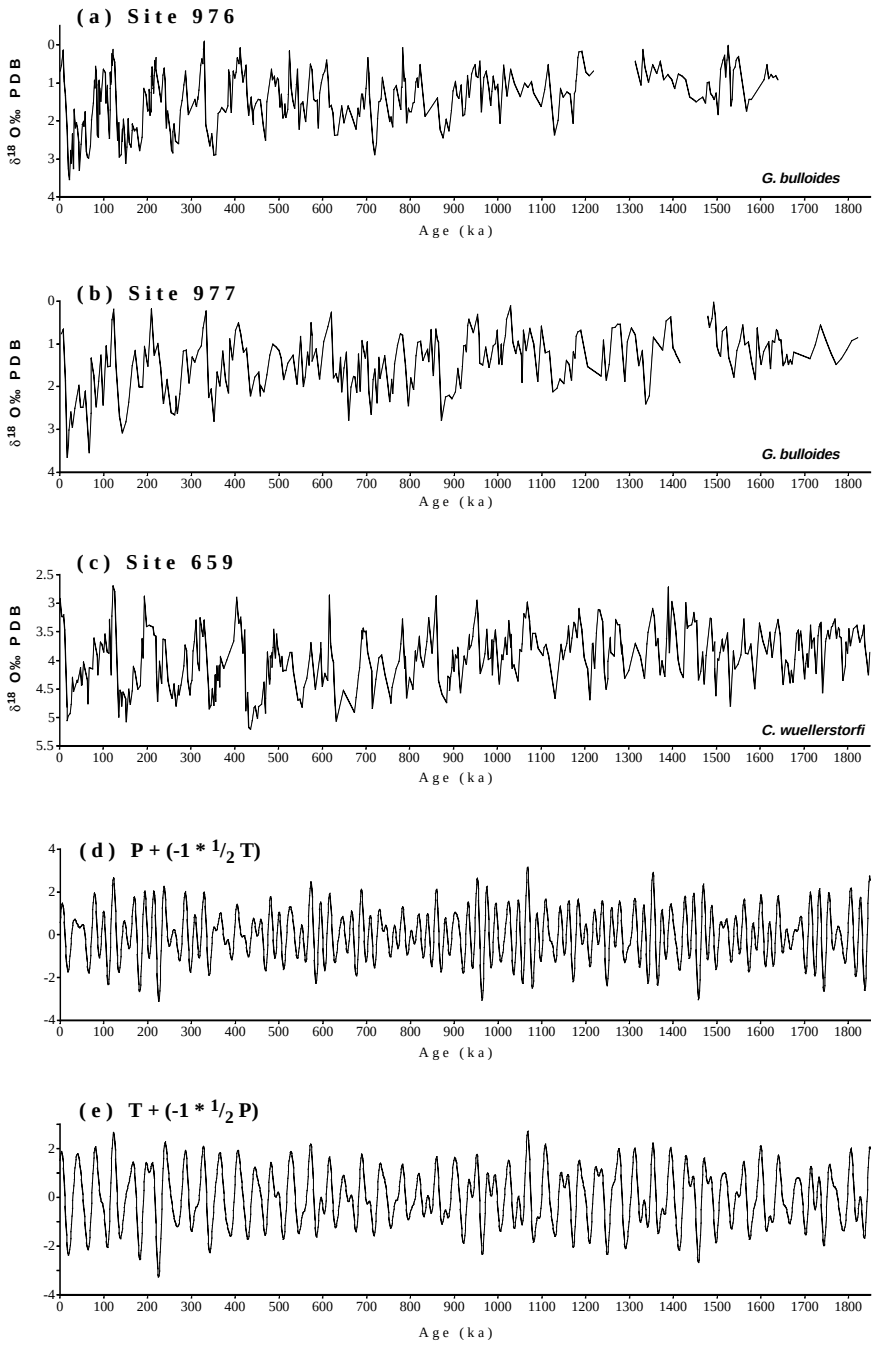

Figure 3. Planktonic δ18O profiles for Sites 976 (**A**) and 977 (**B**) on an age scale. The isotope record of Site 659 (**C**) of Tiedemann et al. (1994) has been used for graphical correlation. The orbital target curves (**D, E**) have been used for fine tuning of the age scales. For discussion see text.

sampled at constant 3-k.y.-age intervals and linearly detrended before spectral analysis. Spectra were run separately on three sections of the records to account for differences in quality and character of the records that would distort the spectra if run on the entire records. The sections follow:

1. 0–430 k.y.; the isotope records show high-amplitude (>2‰ to >3‰) glacial-interglacial δ18O fluctuations that occur at 100-k.y. periods; mean time step in the isotope records is 2.8 k.y. at Site 976 and 5.7 k.y. at Site 977;
2. 430-870 k.y.; δ18O amplitudes are decreased (1.5–2.5‰) and are not as clearly bundled into 100 k.y. cycles as in the upper core section; mean time step in the isotope records is 4.5 k.y. at Site 976 and 5.4 k.y. at Site 977; and
3. >920 k.y.; δ18O amplitudes remain below 1.5‰ and the records show higher-frequency changes that are characteristic for the pre-Brunhes chronozone; for Site 976, the time interval 920–1210 k.y. (mean time step 5.9 k.y.) was analyzed, for Site 977 the time interval 920–1416 k.y. (mean time step 6.5 k.y.). The structure in the earlier sections of both isotope records is inconclusive with respect to the global isotope stratigraphy, and the time models for the earliest parts of the records have been established by using biostratigraphy only i.e., it was not possible to apply orbital tuning.

Numbers of lags for the three time intervals were set to 2/3 of the number of data points in each interval to enhance the resolution of the spectra. Confidence levels of the spectral signals are 80%.

Table 4. Fixpoints for age calibration at Sites 976 and 977.

Site 976		Site 977	
Depth (mcd)	Age (ka)	Depth (mbsf)	Age (ka)
0.00	0.00	2.08	11.50
1.32	4.00	6.76	31.00
2.50	9.00	12.20	57.00
3.30	9.70	13.55	69.60
4.00	11.50	19.73	104.00
5.16	15.60	23.85	124.00
6.40	18.44	30.55	173.00
24.86	63.00	33.00	195.00
27.53	72.30	35.48	213.00
29.46	79.00	39.23	239.00
36.06	113.00	42.10	264.00
43.66	136.00	43.55	268.50
49.66	181.00	52.76	332.00
54.46	205.00	68.07	428.80
58.96	218.30	70.30	454.00
65.26	237.00	71.35	462.00
73.47	260.00	77.34	503.00
76.55	270.54	79.97	517.00
81.07	286.00	81.55	525.00
84.27	310.00	84.75	553.00
92.67	329.00	89.76	575.00
107.07	393.00	92.32	597.00
116.11	423.65	94.69	618.00
118.28	431.00	103.62	666.00
119.75	438.80	109.02	689.00
125.68	470.00	118.59	731.00
143.08	525.00	120.29	752.80
150.48	552.00	123.73	765.00
154.28	573.00	125.30	776.70
168.89	628.00	141.03	862.00
174.09	676.00	148.01	916.00
184.69	719.00	153.81	934.00
194.48	747.29	156.81	962.00
202.10	763.00	159.03	976.00
203.62	777.67	163.32	998.00
205.90	783.00	170.97	1028.00
217.90	822.00	174.26	1048.00
225.30	871.00	177.24	1070.00
228.10	890.00	183.08	1122.00
244.31	962.00	186.20	1150.00
252.31	1006.00	189.40	1169.00
268.57	1121.73	194.20	1186.00
273.71	1172.00	195.71	1235.00
279.51	1186.00	202.24	1276.00
299.51	1361.00	202.95	1281.00
313.12	1473.00	204.64	1298.00
318.38	1493.00	206.52	1315.00
322.92	1516.00	210.00	1343.00
328.32	1533.00	210.80	1349.00
339.98	1569.70	211.31	1364.00
348.63	1613.00	215.16	1397.00
349.32	1619.00	223.19	1428.00
		223.39	1479.00
		231.48	1512.00
		233.55	1529.00
		239.81	1568.00
		242.19	1588.00
		247.51	1614.00
		248.17	1619.00
		255.78	1652.00
		261.78	1677.00
		261.98	1710.00
		262.73	1719.00

Concentration of variance is highest at the main orbital frequencies at Sites 976 and 977 (Fig. 4). The spectral evolution since 1.6 Ma, however, displays interesting differences in the distribution of spectral variance between the eccentricity, obliquity and precession bands. The spectrum of the last 430 k.y. is dominated by the 100-k.y. eccentricity peak in both records. This indicates that cyclic changes in the planktonic oxygen isotope records responded primarily to high-latitude climate forcing associated with a repeated glacial expansion in northern hemisphere ice sheets and sea level variation at the 100-k.y. rhythm. Significant power occurs also at obliquity and precessional periods. At Site 977, the spectral variance is higher at orbital obliquity, whereas the spectral power at orbital precession is higher at Site 976. This difference in spectral character may be a result of differences in stratigraphic resolution between the two isotope records.

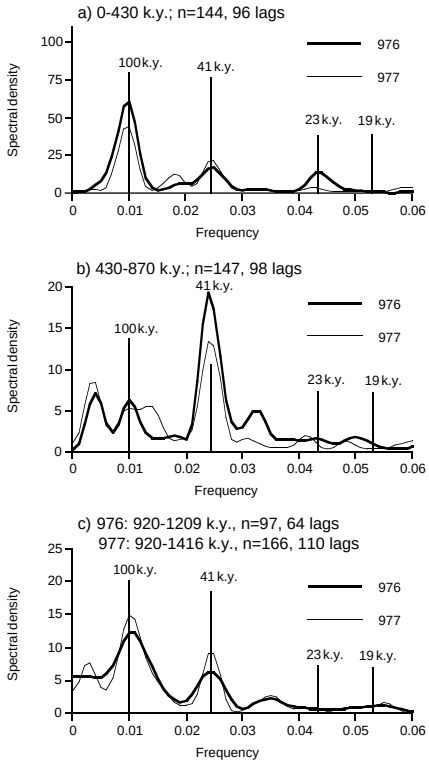

Figure 4. Pleistocene frequency spectra of planktonic isotope records from Sites 976 (thick line) and 977 (thin line) for three time intervals: (**A**) 0–430 k.y., (**B**) 430–870 k.y., (**C**) older than 920 k.y. Vertical lines indicate central frequencies of orbital eccentricity (100 k.y.), obliquity (41 k.y.) and precession (23 k.y., 19 k.y.). To enable a comparison between the three spectra, the number of lags was set to 2/3 of the number of data points (n). See text for discussion.

Spectra for the time interval 430–870 k.y. are dominated by the 41-k.y. obliquity peak, followed by the 100-k.y. eccentricity peak. The 23 and 19-k.y. cycles play only a minor role. This implies that eccentricity signals did not yet dominate western Mediterranean climates during this period. The isotope records at Sites 976 and 977 instead show that the eccentricity period became dominant after 500 k.y. (i.e., 100-200 k.y. later than is observed in isotope records from the open ocean). There, the 100-k.y. power doubled during the period from 780–400 k.y. to 400–0 k.y., with fastest changes around 700–600 k.y. (Ruddiman et al., 1989; Imbrie et al., 1992). The dominance of the 41-k.y. cyclicity suggests that the Mediterranean $\delta^{18}O$ variability was mainly linked to high-latitude climate change (Imbrie et al., 1992).

The frequency spectra for the Pleistocene time interval older than 920 ka are dominated by the 100-k.y. eccentricity period, contrary to the spectral character of isotope records from the open ocean (Ruddiman et al., 1989; Imbrie et al., 1992). This signal is unexpected, and, at least for Site 976, statistically not well constrained in view of the short time interval of only 290 k.y. that was used for spectral analysis. However, for Site 977 the analyzed time interval is 500 k.y., and, in this case, spectral density at the 100-k.y. period is even stronger. However, we cannot exclude the possibility that insufficient sampling resolution mimics a stronger contribution of low-frequency signals that otherwise would fall into the periodicities of obliquity and precession. This would also explain the apparent lack of spectral

power at the precession periods of 23 k.y. and 19 k.y. for both isotope records.

DISCUSSION

The Mediterranean Sea as a semi-enclosed basin has only limited water exchange with the open ocean. Volume transports through the Strait of Gibraltar are largely driven by the Mediterranean's water budget and are limited by the internal hydraulics of the Strait of Gibraltar (Madelain, 1970; Béthoux, 1979; Bryden and Stommel, 1984; Armi and Farmer, 1985; Bryden and Kinder, 1991b). Thus, the Mediterranean acts as a concentration basin in which climate signals become less diluted and are documented in the sediments at much higher resolution than in the open ocean (Thiede, 1978; Thunell and Williams, 1989). Because of the restricted gateway connection with the Atlantic, global sea-level variations exert additional control on the Mediterranean's hydrography (Bryden and Kinder, 1991b).

$\delta^{18}O$ amplitudes in the planktonic isotope records at Site 976 and 977 are high compared to those observed along isotope records from the open ocean. For instance, planktonic isotope records from the Portuguese margin that have been measured using the same planktonic foraminiferal species (*G. bulloides*) display a glacial-interglacial amplitude of $\delta^{18}O$ of 2.6‰ (Bard et al., 1989; Zahn et al., 1997). Glacial-interglacial $\delta^{18}O$ shifts at Sites 976 and 977 are between 3.0‰ and 3.5‰ during the past 450 k.y., pointing to an amplification of climate signals in conjunction with glacial-interglacial sea level changes. These signals likely contain a combination of changing surface water temperature and salinity that was driven by varying rates of precipitation and temperature-salinity variations of inflowing Atlantic waters. Coeval changes of planktonic foraminiferal communities (Linares et al., Chap. 35, this volume; Serrano et al., Chap. 14, this volume) and dinoflagellate evidence at Site 976 (Combourieu Nebout et al., Chap. 36, this volume) support the contention of distinct changes in surface water hydrography.

Thunell and Williams (1989) estimated glacial maximum salinity in the western Mediterranean Sea to be higher than today by 1.2, in addition to the mean ocean salinity increase of ~1 associated with the glacial sea level lowering of 120 m. Using the modern relation between $\delta^{18}O$ of seawater (δ_w) and salinity of 0.27 for Mediterranean waters (Pierre, in press), a glacial salinity increase of 1.2 translates into a δ_w increase by some 0.3‰. That is, 0.3‰ of the observed glacial-interglacial planktonic $\delta^{18}O$ change of 3.0‰–3.5‰ is a result of changes in δ_w and salinity of the western Mediterranean. Subtracting a mean-ocean $\delta^{18}O$ shift of 1.2‰ to account for glacial-interglacial changes in global ice-volume (Labeyrie et al., 1987; Fairbanks, 1989) from the remaining 2.7‰–3.2‰ leaves 1.5‰–2.0‰ for local changes in surface temperature at Site 976 and 977. Assuming a temperature effect on foraminiferal $\delta^{18}O$ of 0.25‰ per 1°C (O'Neil et al., 1969; Shackleton, 1974), one arrives at a local sea surface temperature change of some 6°–8°C at Sites 976 and 977. This amount of glacial cooling is in good agreement with estimates of $5°C < \Delta T < 8°C$ which are derived from planktonic foraminiferal census counts at Site 976 (Donoso, pers. comm., 1997).

High-amplitude $\delta^{18}O$ variations are also observed at the orbital precession period (Fig. 4), demonstrating that the fluctuations of surface hydrography at Sites 976 and 977 are not only driven by longer term glacial-interglacial changes but also by precession-controlled variations of western Mediterranean climate. Abundant evidence exists from eastern Mediterranean core sites and from outcrops in Calabria and Sicily (Southern Italy) that orbital precession exerted primary control on climates and hydrography of the eastern Mediterranean during Pliocene–Pleistocene times (Hilgen, 1991a; Hilgen, 1991b; Lourens et al., 1992; van Os et al., 1994). Together with data from long pollen records from Greece (Mommersteg et al., 1995) it was concluded that the principal climate signal at this orbital period is a change from cold/dry to warm/wet conditions (Rossignol-Strick, 1985; Rohling, 1991; Rohling and Bryden, 1994). The fact that similar cyclicities are observed at Sites 976 and 977 in the far western Mediterranean provides clear evidence for the influence of precession on Mediterranean-wide climate and surface hydrography. Yet, climate forcing likely was different for the eastern and western Mediterranean region. In the east, precession-driven variations in monsoonal strength are believed to be the primary climatic component that determines the regional freshwater flux, both by way of enhanced runoff of the Nile river (Rossignol-Strick, 1985) and by stronger precipitation over the northern Mediterranean borderlands during periods of precession minima (Rohling and Gieskes, 1989; Rohling and Bryden, 1994).

In the western Mediterranean Sea, climate change is more closely linked to North Atlantic climates. Varying rates of convective overturn in the northern North Atlantic determine the rate of oceanic heat transport from the tropical-subtropical to the high-latitude North Atlantic, thereby defining the state of regional climate (Broecker et al., 1990; Lehman and Keigwin, 1992; Mikolajewicz and Maier-Reimer, 1994; Sarnthein and Altenbach, 1995; Macdonald and Wunsch, 1996; Seidov and Maslin, 1996; Yu et al., 1996). The $\delta^{18}O$ record at the higher-resolution Site 976 shows considerable variability on sub-Milankovitch time scales (i.e., faster than what would be expected from precessional forcing alone [Fig. 5]). This is best documented for the upper part of the record where sample resolution was highest. Sub-Milankovitch changes of ocean circulation are also documented for the northern North Atlantic. Abrupt changes of conveyor-belt circulation punctuated North Atlantic circulation during the last glacial and resulted in rapid oscillations between polar and subpolar/boreal conditions, as is documented in Greenland ice core records (Dansgaard et al., 1993; Grootes et al., 1993; Taylor et al., 1993) and in paleoceanographic proxy records from open North Atlantic sediment cores (Bond et al., 1993; Grousset et al., 1993; Sarnthein et al., 1994; Fronval et al., 1995; Rasmussen et al., 1996; Zahn et al., 1997). Part of the climatic and oceanic variability conceivably is driven by varying zonality of low-latitude winds and associated changes in advection of subtropical waters and oceanic heat to the northern North Atlantic (McIntyre and Molfino, 1996). In addition, varying rates of glacial ice melt runoff in conjunction with varying

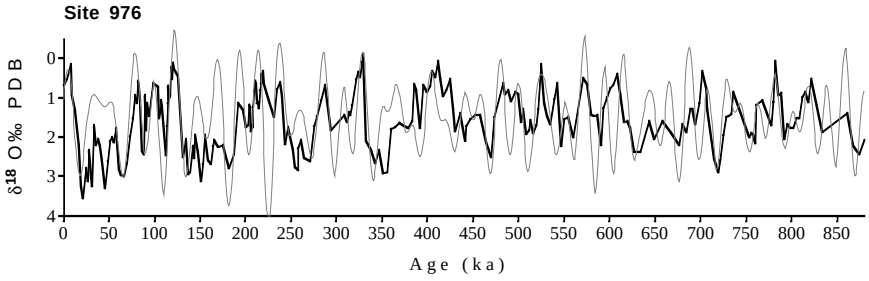

Figure 5. $\delta^{18}O$ record at Site 976 for the last 870 k.y. The isotope record shows considerable variability on sub-Milankovitch scales that are not caused by orbital forcing. The stippled curve is the orbital target curve consisting of normalized precession and one-half normalized obliquity (see Fig. 3).

modes of ice sheet stability (Alley and MacAyeal et al., 1994) would exert additional control on thermohaline overturn in the North Atlantic (Maslin et al., 1995; Zahn et al., 1997).

Climate signals from the North Atlantic region would influence western Mediterranean climates through two pathways: by way of inflowing North Atlantic surface waters whose T-S structure is determined by the thermal history and the history of evaporation and precipitation of the North Atlantic region; and through changes of atmospheric circulation driven by changes in atmospheric pressure gradients over the North Atlantic. Glacial-interglacial changes of surface hydrography along the western Iberian margin are documented in sediment cores from beneath the Portugal current. They show that glacial-maximum surface waters there were colder by 12°C and more saline by 2 salinity units (Bard et al., 1989; Zahn et al., 1997). During mean glacial conditions before the glacial-maximum period, temperature was 4°C lower than today and salinity close to the modern level. The abrupt anomalies that punctuated North Atlantic climate during the last glacial were associated with temperature and salinity decreases of 8°C and 1–2 salinity units, respectively, in the Portugal current. Today, and most likely also during glacial periods, the Atlantic inflow to the Mediterranean is driven from the Portugal current and thus, the hydrographic signals that are documented at the western Iberian margin likely were advected into the Alboran Sea with the Atlantic surface inflow.

Atmospheric circulation over the North Atlantic is modulated by the North Atlantic Oscillation (NAO), which is driven by meridional pressure gradients between the boreal North Atlantic region and subantarctic latitudes (Hurrell, 1995). Changes in atmospheric circulation associated with changes of the NAO index determine the latitudinal position of North Atlantic depression tracks that carry enhanced amounts of moisture to the east. In the event of strong latitudinal pressure gradients (high NAO index), the depression tracks follow a more northerly path across central and northern Europe. Decreased latitudinal pressure gradients (low NAO index) drive the depression tracks along a more southerly position across the Mediterranean.

Diversion of atmospheric moisture flux from northern Europe and Scandinavia to southern Europe and the Mediterranean thus is a viable mechanism to alter the Mediterranean's freshwater budget. At this point it is not possible to distinguish in detail between the signals that are driven by the Atlantic inflow and those that result from changes in North Atlantic atmospheric circulation. In spite of this, we use the high-amplitude $\delta^{18}O$ fluctuations at Site 976 and 977 that occur primarily at the orbital precession period as an indication for rhythmic incursions of periods with excess precipitation. These periods were not strictly linked to glacial-interglacial climates but were driven by changes in atmospheric circulation in conjunction with changes similar to today's North Atlantic Oscillation.

Comparison of the planktonic $\delta^{18}O$ records at Sites 976 and 977 with the orbital insolation curve (Laskar et al., 1993) shows that the negative $\delta^{18}O$ excursions closely correlate with periods of maximum northern hemisphere summer insolation (Fig. 6). Insolation maxima occur at a period of the orbital precession and were used to infer climatic conditions that were favorable for the formation of sapropels in the eastern Mediterranean (Rohling and Gieskes, 1989; Emeis et al., 1991; Hilgen, 1991a; Lourens et al., 1992; Rohling, 1994; van Os et al., 1994). At Sites 976 and 977, some organic-rich layers (ORLs; defined as containing organic carbon concentrations above background; see Murat, Chap. 41, this volume) indeed occur during or close to periods of maximum summer insolation and minimum planktonic $\delta^{18}O$. However, detailed stratigraphic correlation suggests that most ORLs at Sites 976 and 977 are not related to insolation maximum but their stratigraphic distribution appears to be unsystematic in that they were deposited during full glacial and deglacial periods (Fig. 6). This suggests that, in addition to orbital forcing, independent mechanisms existed in the Alboran Sea that stimulated primary productivity and/or enhanced organic carbon preservation at both sites. Variable strength of the Atlantic jet-like inflow and local upwelling fronts that are associated with it (Tintoré et al., 1994) are likely candidates for periodic enhancement of biological productivity.

SUMMARY AND CONCLUSIONS

Planktonic $\delta^{18}O$ profiles measured on *G. bulloides* were established for the Pleistocene sections of Sites 976 and 977. The sites are in the Alboran Sea, close to the gateway for Atlantic-Mediterranean

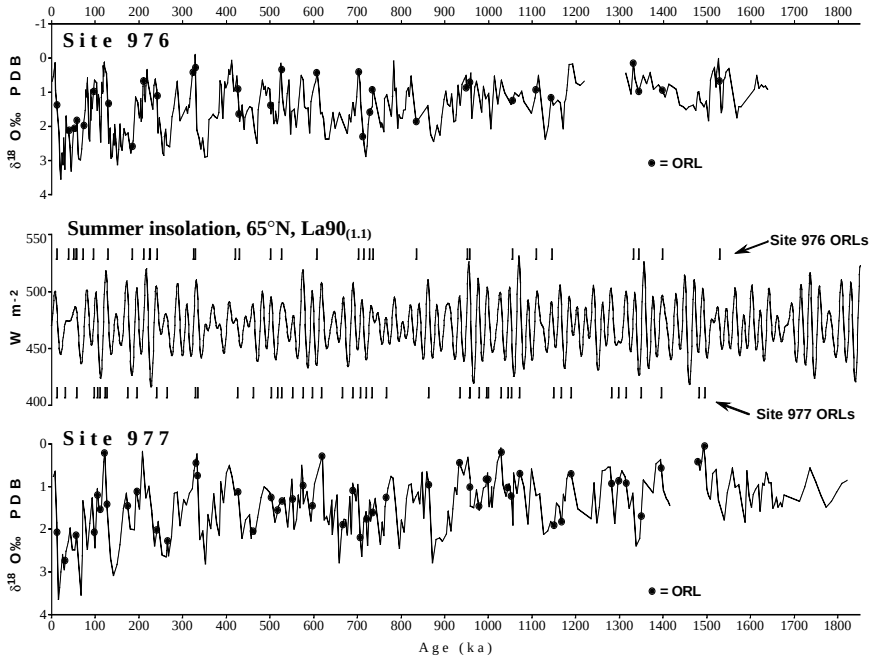

Figure 6. The $\delta^{18}O$ records at Sites 976 (top panel) and 977 (bottom panel) and the orbital insolation record after Laskar et al. (1993). Full dots indicate the position of organic rich layers (ORL; Murat, Chap. 41, this volume). The occurrence of the ORLs is not exclusively linked to insolation maxima and $\delta^{18}O$ minima. ORLs apparently occur irregularly and likely are linked to shifts in position of the Atlantic jet-like inflow that generates local upwelling fronts in the Alboran Sea. See text for discussion.

water exchange. Both sites are at the westernmost extension of the Legs 160/161 trans-Mediterranean drilling transect that was designed to extend our knowledge about the paleoclimatic and oceanographic history of the Mediterranean Sea.

The age models were developed using biostratigraphic marker events (de Kaenel et al., Chap. 13, this volume) and graphical correlation to the Site 659 isotope curve of Tiedemann et al. (1994). For final fine-tuning, two insolation target curves were constructed with variable inputs of precession and obliquity components. According to the age models, the $\delta^{18}O$ records reach back to 1.4 Ma (Site 976) and 1.7 Ma (Site 977). Sedimentation rates are 15–40 cm/k.y., allowing for high-resolution paleoclimate records. Glacial-interglacial amplitudes of $\delta^{18}O$ are 3.0-3.5‰ and are amplified above the global average, thus pointing to significant variation of regional temperature and salinity. High-frequency variations on sub-Milankovitch time scales occur throughout the records and point to additional forcing outside orbitally modulated climate change.

Power spectra of the $\delta^{18}O$ records show variable dominance of the main orbital cycles over time. From 0 to 430 k.y. the 100-k.y. cycle of eccentricity is dominant at both sites, but significant power also occurs for the obliquity cycle of 40-k.y. and the precession cycle of 20 k.y. Between 430 and 870 k.y. the 40-k.y. cycle is dominant, while the 100-k.y. cycle plays only a minor role. The mid-Pleistocene strong influence of the eccentricity cycle seems to start some 100 to 200 k.y. later in the Mediterranean than elsewhere. Before 920 ka the 100- and 40-k.y. cycles show the strongest power, but the dominance of 100-k.y. cycles in the early Pleistocene sections of both records likely is a result of insufficient time resolution, so that precessional signals not resolved adequately.

Horizons of enhanced organic carbon concentrations (organic-rich layers [ORLs]; Murat, Chap. 41, this volume) do not strictly correlate with periods of minimum planktonic $\delta^{18}O$ and maximum insolation. Comparison with the orbital insolation record demonstrates that most ORLs at Site 976 and 977 were deposited during periods of only moderate or even minimum insolation. Only a few ORLs directly correlate with insolation maxima. This pattern is different from that of type sapropels in the eastern Mediterranean that closely correlate with periods of moist and warm climates (i.e., insolation maxima). At Sites 976 and 977, variable strength or shifts in position of local upwelling fronts that are associated with the jet-like Atlantic inflow may have played a primary role in causing the deposition of organic-rich facies. Such variations were conceivably linked to changes in North Atlantic climates and concomitant changes in the Atlantic inflow and atmospheric circulation.

ACKNOWLEDGMENTS

We thank N. Nebout Combourieu, L. Vigliotti, L. Capotondi, and P. Belanger for stimulating discussions. E. de Kaenel improved the biostratigraphy at Sites 976 and 977 and helped to resolve differences between the isotopic and biostratigraphic time scales. M. Cita, L. Lourens, and an anonymous reviewer provided helpful comments to improve the manuscript. W. Hale and his staff at the Bremen Core Repository helped us to sample the cores and to organize the sampling party. The Bremen Core Repository is jointly funded by the Ocean Drilling Program, the University of Bremen, and the Deutsche Forschungsgemeinschaft. This work was supported by the Deutsche Forschungsgemeinschaft under grant Za 157/10.

REFERENCES

Abrantes, F., 1988. Diatom productivity peak and increased circulation during the latest Quaternary: Alboran Basin (western Mediterranean). *Mar. Micropaleontol.*, 13:79–96.

Alley, R.B., and MacAyeal, D.R., 1994. Ice-rafted debris associated with binge/purge oscillations of the Laurentide Ice Sheet. *Paleoceanography*, 9:503–511.

Armi, L., and Farmer, D., 1985. The internal hydraulics of the Strait of Gibraltar and associated sills and narrows. *Oceanol. Acta*, 8:37–46.

Bard, E., Fairbanks, R., Arnold, M., Maurice, P., Duprat, J., Moyes, J., and Duplessy, J.-C., 1989. Sea-level estimates during the last deglaciation based on $\delta^{18}O$ and accelerator mass spectrometry ^{14}C ages measured in *Globigerina bulloides*. *Quat. Res.*, 31:381–391.

Béthoux, J.P., 1979. Budgets of the Mediterranean Sea: their dependence on the local climate and the characteristics of the Atlantic waters. *Oceanol. Acta.*, 2:157–163.

————, 1984. Paléo-hydrologie de la Méditerranée au cours derniers 20000 ans. *Oceanol. Acta*, 7:43–48.

Bond, G., Broecker, W., Johnsen, S., McManus, J., Labeyrie, L., Jouzel, J., and Bonani, G., 1993. Correlations between climate records from the North Atlantic sediments and Greenland ice. *Nature*, 365:143–147.

Bray, N.A., Ochoa, J., and Kinder, T.H., 1995. The role of the interface in exchange through the Strait of Gibraltar. *J. Geophys. Res.*, 100:10755–10776.

Broecker, W.S., Bond, G., Klas, M., Bonani, G., and Wolfi, W., 1990. A salt oscillator in the glacial Atlantic? 1. The concept. *Paleoceanography*, 5:469–477.

Bryden, H.L., and Kinder, T.H., 1991a. Recent progress in strait dynamics. *Rev. Geophys., Suppl., (U.S. Nat. Rep. Int. Union Geodesy Geophys. 1987–1990)*, 617–631.

————, 1991b. Steady two-layer exchange through the Strait of Gibraltar. *Deep-Sea Res.*, 38:445–463.

Bryden, H.L., and Stommel, H.M., 1984. Limiting processes that determine basic features of the circulation in the Mediterranean Sea. *Oceanol. Acta*, 7:289–296.

Calvert, S.E., Nielsen, B., and Fontugne, M.R., 1992. Evidence from nitrogen isotope ratios for enhanced productivity during the formation of eastern Mediterranean sapropels. *Nature*, 359:223–225.

Caralp, M.-H., 1988. Late Glacial to Recent deep-sea benthic foraminifera from the northeastern Atlantic (Cadiz Gulf) and western Mediterranean (Alboran Sea): paleoceanographic results. *Mar. Micropaleontol.*, 13:265–289.

Cita, M.B., Broglia, C., Malinverno, A., Spezzibottiani, G., Tomadin, L., and Violanti, D., 1982. Late Quaternary pelagic sedimentation on the southern Calabrian Ridge and western Mediterranean Ridge, Eastern Mediterranean. *Mar. Micropaleontol.*, 7:135–162.

Cita, M.B., Vergnaud-Grazzini, C., Robert, C., Chamley, H., Ciaranfi, N., and D'Onofrio, S., 1977. Paleoclimatic record of a long deep sea core from the eastern Mediterranean. *Quat. Res.*, 8:205–235.

Comas, M.C., Zahn, R., Klaus, A., et al., 1996. *Proc. ODP, Init. Repts.*, 161: College Station, TX (Ocean Drilling Program).

Dansgaard, W., Johnsen, S.J., Clausen, H.B., Dahl-Jensen, D., Gundestrup, N.S., Hammer, C.U., Hvidberg, C.S., Steffensen, J.P., Sveinbjörnsdottir, A.E., Jouzel, J., and Bond, G., 1993. Evidence for general instability of past climate from a 250-kyr ice-core record. *Nature*, 364:218–220.

Donde Va Group, 1984. Donde Va? An oceanographic experiment in the Alboran Sea. *Eos*, 65:682–683.

Emeis, K.-C., Camerlenghi, A., McKenzie, J.A., Rio, D., and Sprovieri, R., 1991. The occurrence and significance of Pleistocene and Upper Pliocene sapropels in the Tyrrhenian Sea. *Mar. Geol.*, 100:155–182.

Fairbanks, R.G., 1989. A 17,000-year glacio-eustatic sea level record: influence of glacial melting rates on the Younger Dryas event and deep-ocean circulation. *Nature*, 342:637–642.

Fronval, T., Jansen, E., Bloemendal, J., and Johnsen, S., 1995. Oceanic evidence for coherent fluctuations in Fennoscandian and Laurentide ice sheets on millennium timescales. *Nature*, 374:443–446.

Gascard, J.-C., 1978. Mediterranean deep water formation, baroclinic instability and oceanic eddies. *Oceanol. Acta*, 1:315–330.

Grootes, P.M., Stuvier, M., White, J.W.C., Johnsen, S., and Jouzel, J., 1993. Comparison of oxygen isotope records from the GISP2 and GRIP Greenland ice cores. *Nature*, 366:552–554.

Grousset, F.E., Joron, J.L., Biscaye, P.E., Latouche, C., Treuil, M., Maillet, N., Faugeres, J.C., and Gonthier, E., 1988. Mediterranean outflow through the Strait of Gibraltar since 18,000 years B.P.: mineralogical and geochemical arguments. *Geo-Mar. Lett.*, 8:25–34.

Grousset, F.E., Labeyrie, L., Sinko, J.A., Cremer, M., Bond, G., Duprat, J., Cortijo, E., and Huon, S., 1993. Patterns of ice-rafted detritus in the glacial North Atlantic (40°–55°N). *Paleoceanography,* 8:175–192.

Hilgen, F.J., 1991a. Astronomical calibration of Gauss to Matuyama sapropels in the Mediterranean and implication for the geomagnetic polarity time scale. *Earth Planet. Sci. Lett.,* 104:226–244.

————, 1991b. Extension of the astronomically calibrated (polarity) time scale to the Miocene/Pliocene boundary. *Earth Planet. Sci. Lett.,* 107:349–368.

Hilgen, F.J., Lourens, L.J., Berger, A., and Loutre, M.F., 1993. Evaluation of the astronomically calibrated timescale for the late Pliocene and earliest Pleistocene. *Paleoceanography,* 8:549–565.

Hurrell, J.W., 1995. Decadal trends in the North Atlantic Oscillation: regional temperatures and precipitation. *Science,* 269:676–679.

Imbrie, J., Boyle, E.A., Clemens, S.C., Duffy, A., Howard, W.R., Kukla, G., Kutzbach, J., Martinson, D.G., McIntyre, A., Mix, A.C., Molfino, B., Morley, J.J., Peterson, L.C., Pisias, N.G., Prell, W.L., Raymo, M.E., Shackleton, N.J., and Toggweiler, J.R., 1992. On the structure and origin of major glaciation cycles, 1. Linear responses to Milankovitch forcing. *Paleoceanography,* 7:701–738.

Imbrie, J., and Imbrie, J.Z., 1980. Modeling the climatic response to orbital variations. *Science,* 207:943–953.

Kullenberg, B., 1952. On the salinity of the water contained in marine sediments. *Goeteborgs K. Vetensk. Vitterhets-Samh. Handl., Ser. B,* 6:3–37.

Labeyrie, L.D., Duplessy, J.C., and Blanc, P.L., 1987. Variations in mode of formation and temperature of oceanic deep waters over the past 125,000 years. *Nature,* 327:477–482.

Lacombe, H., 1984. General physical oceanography of the Mediterranean Sea. *Proc. NATO Adv. Res. Workshop*.

Lacombe, H., and Richez, C., 1982. The regime of the Strait of Gibraltar. *In* Nihoul, J.C.J. (Ed.), *Hydrodynamics of Semi-enclosed Seas*: New York (Elsevier), 13–74.

Lascaratos, A., Williams, R.G., and Tragou, E., 1993. A mixed-layer study of the Levantine intermediate water. *J. Geophys. Res.,* 98:14739–14749.

Laskar, J., Joutel, F., and Boudin, F., 1993. Orbital, precessional, and insolation quantities for the Earth from –20 Myr to +10 Myr. *Astron. Astrophys.,* 270:522–533.

La Violette, P.E., 1990. The western Mediterranean circulation experiment (WMCE): introduction. *J. Geophys. Res.,* 95:1511–1514.

La Violette, P.E. (Ed.), 1994. *Seasonal and Interannual Variability of the Western Mediterranean Sea:* Washington (Am. Geophys. Union), Coastal and Estuarine Studies, 46.

Lehman, S.J., and Keigwin, L.D., 1992. Sudden changes in North Atlantic circulation during the last deglaciation. *Nature,* 356:757–762.

Lourens, L.J., Antonarakou, A., Hilgen, F.J., Van Hoof, A.A.M., Vergnaud-Grazzini, C., and Zachariasse, W.J., 1996. Evaluation of the Plio-Pleistocene astronomical timescale. *Paleoceanography,* 11:391–413.

Lourens, L.J., Hilgen, F.J., Gudjonsson, L., and Zachariasse, W.J., 1992. Late Pliocene to early Pleistocene astronomically forced sea surface productivity and temperature variations in the Mediterranean. *Mar. Micropaleontol.,* 19:49–78.

Macdonald, A.M., and Wunsch, C., 1996. An estimate of global ocean circulation and heat fluxes. *Nature,* 382:436–439.

Madelain, F., 1970. Influence de la topographie du fond sur l'écoulement méditerranéen entre le Détroit de Gibraltar et le Cap Saint-Vincent. *Cah. Océanogr.,* 22:43–61.

Maslin, M.A., Shackleton, N., and Pflaumann, U., 1995. Surface water temperature, salinity and density changes in the N.E. Atlantic during the last 45,000 years: Heinrich events, deep water formation and climatic rebounds. *Paleoceanography,* 10:527–544.

McIntyre, A., and Molfino, B., 1996. Forcing of Atlantic equatorial and subpolar millenial cycles by precession. *Science,* 274:1867–1870.

MEDOC Group, 1970. Observation of formation of deep water in the Mediterranean Sea. *Nature,* 227:1037–1040.

Mikolajewicz, U., and Maier-Reimer, E., 1994. Mixed boundary conditions in ocean general circulation models and their influence on the stability of the model's conveyor belt. *J. Geophys. Res.,* 99:633–644.

Millot, C., 1987. Circulation in the western Mediterranean Sea. *Oceanol. Acta,* 10:143–149.

Mix, A.C., Pisias, N.G., Rugh, W., Wilson, J., Morey, A., and Hagelberg, T.K., 1995. Benthic foraminiferal stable isotope record from Site 849: 0–5 Ma: local and global climate changes. *In* Pisias, N.G., Mayer, L.A., Janecek, T.R., Palmer-Julson, A., and van Andel, T.H. (Eds.), *Proc. ODP, Sci. Results,* 138: College Station, TX (Ocean Drilling Program), 371–412.

Mommersteg, H.J.P.M., Loutre, M.F., Young, R., Wijmstra, T.A., and Hooghiemstra, H., 1995. Orbital forced frequencies in the 975,000 year pollen record from Tenagi Philippon (Greece). *Clim. Dyn.,* 11:4–24.

Olausson, E., 1961. Studies of deep-sea cores. *Rep. Swed. Deep-Sea Exped., 1947–1948,* 8:335–391.

O'Neil, J.R., Clayton, R.N., and Mayeda, T.K., 1969. Oxygen isotope fractionation in divalent metal carbonates. *J. Chem. Phys.,* 51:5547–5558.

Paillard, D., Labeyrie, L., and Yiou, P., 1996. Macintosh program performs time-series analysis. *Eos,* 77:379.

Pierre, C., in press. The oxygen and carbon isotope distribution in the Mediterranean water masses. *Mar. Geol.*

Rasmussen, T.L., Thomsen, E., van Weering, T.C.E., and Labeyrie, L., 1996. Rapid changes in surface and deepwater-conditions at the Faeroe Margin during the last 58,000 years. *Paleoceanography,* 11:757–771.

Reid, J.L., 1979. On the contribution of the Mediterranean Sea outflow to the Norwegian-Greenland Sea. *Deep-Sea Res. Part A,* 26:1199–1223.

Rohling, E.J., 1991. Shoaling of the Eastern Mediterranean pycnocline due to reduction of excess evaporation: implications for sapropel formation. *Paleoceanography,* 6:747–753.

————, 1994. Review and new aspects concerning the formation of eastern Mediterranean sapropels. *Mar. Geol.,* 122:1–28.

Rohling, E.J., and Gieskes, W.W.C., 1989. Late Quaternary changes in Mediterranean intermediate water density and formation rate. *Paleoceanography,* 4:531–545.

Rohling, E.J., and Hilgen, F.J., 1991. The eastern Mediterranean climate at times of sapropel formation: a review. *Geol. Mijnbouw,* 70:253–264.

Rohling, E.J., and Bryden, H.L., 1992. Man-induced salinity and temperature increases in the western Mediterranean deep water. *J. Geophys. Res.,* 97:11191–11198.

————, 1994. Estimating past changes in the eastern Mediterranean freshwater budget, using reconstructions of sea-level and hydrography. *Proc. Kon. Neder. Akad. Wetensch. B,* 97:201–217.

Rohling, E.J., Den Dulk, M., Pujol, C., and Vergnaud-Grazzini, C., 1995. Abrupt hydrographic change in the Alboran Sea (western Mediterranean) around 8000 yrs BP. *Deep-Sea Res.,* 42:1609–1619.

Rossignol-Strick, M., 1985. Mediterranean Quaternary sapropels, an immediate response of the African Monsoon to variation of insolation. *Palaeogeogr., Palaeoclimatol., Palaeoecol.,* 49:237–263.

Ruddiman, W.F., Raymo, M.E., Martinson, D.G., Clement, B.M., and Backman, J., 1989. Pleistocene evolution: Northern Hemisphere ice sheets and North Atlantic Ocean. *Paleoceanography,* 4:353–412.

Ryan, W.B.F., Hsü, K.J., et al., 1973. *Init. Repts. DSDP,* 13 (Pts. 1 and 2): Washington (U.S. Govt. Printing Office).

Sarmiento, J., Herbert, T., and Toggweiler, J., 1988. Mediterranean nutrient balance and episodes of anoxia. *Global Biogeochem. Cycles,* 2:427–444.

Sarnthein, M., and Altenbach, A.V., 1995. Late Quaternary changes in surface water and deep water masses of the Nordic Seas and northern North Atlantic: a review. *Geol. Rundsch.,* 84:89–107.

Sarnthein, M., Winn, K., Jung, S., Duplessy, J.-C., Labeyrie, L., Erlenkeuser, H., and Ganssen, G., 1994. Changes in East Atlantic deep-water circulation over the last 30,000 years: eight time slice reconstructions. *Paleoceanography,* 9:209–267.

Seidov, D., and Maslin, M., 1996. Seasonally ice free glacial Nordic seas without deep water ventilation. *Terra Nova,* 8:245–254.

Shackleton, N.J., 1974. Attainment of isotopic equilibrium between ocean water and the benthonic foraminifera genus *Uvigerina:* isotopic changes in the ocean during the last glacial. *Les Meth. Quant. d'étude Var. Clim. au Cours du Pleist., Coll. Int. C.N.R.S.,* 219:203–209.

Shackleton, N.J., Berger, A., and Peltier, W.A., 1990. An alternative astronomical calibration of the lower Pleistocene timescale based on ODP Site 677. *Trans. R. Soc. Edinburgh: Earth Sci.,* 81:251–261.

Stanley, D. J., 1978. Ionian Sea sapropel distribution and late Quaternary palaeoceanography in the eastern Mediterranean. *Nature,* 274:149–152.

Taylor, K.C., Hammer, C.U., Alley, R.B., Clausen, H.B., Dahl-Jensen, D., Gow, A.J., Gundestrup, N.S., Kipfstuhl, J., Moore, J.C., and Waddington, E.D., 1993. Electrical conductivity measurements from the GISP2 and GRIP Greenland ice cores. *Nature,* 366:549–552.

Thiede, J., 1978. A glacial Mediterranean. *Nature,* 276:680–683.

Thunell, R.C., and Williams, D.F., 1989. Glacial-Holocene salinity changes in the Mediterranean Sea: hydrographic and depositional effects. *Nature,* 338:493–496.

Tiedemann, R., Sarnthein, M., and Shackleton, N.J., 1994. Astronomic timescale for the Pliocene Atlantic $\delta^{18}O$ and dust flux records of Ocean Drilling Program Site 659. *Paleoceanography,* 9:619–638.

Tintoré, J., Viúdez, A., Gomis, D., Alonso, S., and Werner, F.E., 1994. Mesoscale variability and Q vector vertical motion in the Alboran Sea. *In* La Violette, P.E. (Ed.), *Seasonal and Interannual Variability of the Western Mediterranean Sea:* Washington (Am. Geophys. Union), Coastal and Estuarine Studies, 46:47–71.

Troelstra, S.R, and van Hinte, J.E., 1995. The Younger Dryas-Sapropel S1 connection in the Mediterranean Sea (extended Abstract). *Geol. Mijnbouw,* 74:275–280.

Van Os, B.J.H., Lourens, L.J., Hilgen, F.J., De Lange, G.J., and Beaufort, L., 1994. The formation of Pliocene sapropels and carbonate cycles in the Mediterranean: diagenesis, dilution, and productivity. *Paleoceanography,* 9:601–617.

Vergnaud-Grazzini, C., Devaux, M., and Znaidi, J., 1986. Stable isotope "anomalies" in Mediterranean Pleistocene records. *Mar. Micropaleontol.,* 10:35–69.

Vergnaud-Grazzini, C., and Pierre, C., 1991. High fertility in the Alboran Sea since the Last Glacial Maximum. *Paleoceanography,* 6:519–536.

Vergnaud-Grazzini, C., Ryan, W.B.F., and Cita, M.B., 1977. Stable isotope fractionation, climatic change and episodic stagnation in the Eastern Mediterranean during the Late Quaternary. *Mar. Micropaleontol.,* 2:353–370.

Williams, D.F., Thunell, R.C., and Kennett, J.P., 1978. Periodic freshwater flooding and stagnation of the eastern Mediterranean Sea during the late Quaternary. *Science,* 201:252–254.

Wu, P., and Haines, K., 1996. Modeling the dispersal of Levantine Intermediate Waters and its role in Mediterranean deep water formation. *J. Geophys. Res.,* 101:6591–6607.

Wüst, G., 1961. On the vertical circulation of the Mediterranean Sea. *J. Geophys. Res.,* 66:3261–3271.

Yu, E.F., Francois, R., and Bacon, M.P., 1996. Similar rates of modern and last-glacial ocean thermohaline circulation inferred from radiochemical data. *Nature,* 379:689–694.

Zahn, R., Sarnthein, M., and Erlenkeuser, H., 1987. Benthic isotope evidence for changes of the Mediterranean outflow during the late Quaternary. *Paleoceanography,* 2:543–559.

Zahn, R., Schönfeld, J., Kudrass, H.-R., Park, M.-H., Erlenkeuser, H., and Grootes, P., 1997. Thermohaline instability in the North Atlantic during meltwater events: stable isotope and ice rafted detritus records from core SO75-26KL, Portuguese margin. *Paleoceanography,* 12: 696–710.

Zenk, W., Schultz Tokos, K., and Boebel, O., 1992. New observations of meddy movement south of the Tejo Plateau. *Geophys. Res. Lett.,* 19:2389–2392.

Date of initial receipt: 12 May 1997
Date of acceptance: 16 February 1998
Ms 161SR-233